Detection of Temporal Change of Fishery and Island Activities by DNB and SAR on the South China Sea

I. Asanuma, T. Yamaguchi, J. Park, K. J. Mackin

Abstract—Fishery lights on the surface could be detected by the Day and Night Band (DNB) of the Visible Infrared Imaging Radiometer Suite (VIIRS) on the Suomi National Polar-orbiting Partnership (Suomi-NPP). The DNB covers the spectral range of 500 to 900 nm and realized a higher sensitivity. The DNB has a difficulty of identification of fishing lights from lunar lights reflected by clouds, which affects observations for the half of the month. Fishery lights and lights of the surface are identified from lunar lights reflected by clouds by a method using the DNB and the infrared band, where the detection limits are defined as a function of the brightness temperature with a difference from the maximum temperature for each level of DNB radiance and with the contrast of DNB radiance against the background radiance. Fishery boats or structures on islands could be detected by the Synthetic Aperture Radar (SAR) on the polar orbit satellites using the reflected microwave by the surface reflecting targets. The SAR has a difficulty of tradeoff between spatial resolution and coverage while detecting the small targets like fishery boats. A distribution of fishery boats and island activities were detected by the scan-SAR narrow mode of Radarsat-2, which covers 300 km by 300 km with various combinations of polarizations. The fishing boats were detected as a single pixel of highly scattering targets with the scan-SAR narrow mode of which spatial resolution is 30 m. As the look angle dependent scattering signals exhibits the significant differences, the standard deviations of scattered signals for each look angles were taken into account as a threshold to identify the signal from fishing boats and structures on the island from background noise. It was difficult to validate the detected targets by DNB with SAR data because of time lag of observations for 6 hours between midnight by DNB and morning or evening by SAR. The temporal changes of island activities were detected as a change of mean intensity of DNB for circular area for a certain scale of activities. The increase of DNB mean intensity was corresponding to the beginning of dredging and the change of intensity indicated the ending of reclamation and following constructions of facilities.

Keywords—Day night band, fishery, SAR, South China Sea.

I. Introduction

THE South China Sea (SCS) is the second largest semi-enclosed sea in the world [1] holding a large marine ecosystem with the terrestrial inputs from rivers, where fishery activities are deployed widely in the coastal waters and transboundary waters (Fig. 1).

Ichio Asanuma is with Tokyo University of Information Sciences, Chiba, Japan 265-8501 (phone: +81-43-236-4633; e-mail: asanuma@rsch.tuis.ac.jp). Takashi Yamaguchi, Jong-Geol Park and Keneth J. Mackin are with Tokyo University of Information Sciences, Chiba, Japan 265-8501 (e-mail: tyamagu@rsch.tuis.ac.jp, amon@rsch.tuis.ac.jp, mackin@rsch.tuis.ac.jp).

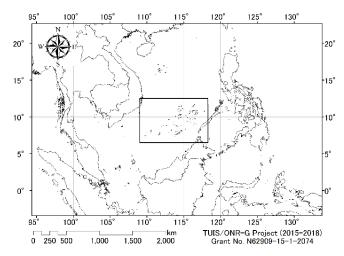


Fig. 1 Spratoly Islands (rectangle region) on the SCS [2]

The DNB of VIIRS on the Suomi-National Polar orbiting Partnership (S-NPP) provides a panchromatic image of the surface in the night, integrating from 500 to 900 nm [3]. The DNB is operated with three gains and the vicarious calibrations have been reported to keep a consistent use of data [4]. The radiance observed by DNB is in the range of the minimum radiance of 3 nW cm⁻² sr⁻¹, which is a sufficient signal to noise ratio, and to the maximum radiance of 100 nW cm⁻² sr⁻¹, which is the saturation level of DNB [5]. The DNB has a wide variety of applications from this optical property [6]. The DNB data were applied to the analysis of urban activities from street lights [4], [5], [7], [8], the recognition of fishing boats from lights for fishing [9]-[11], and the metrological application with clouds distribution associated with fronts and typhoons [4], [8], [9]. First two applications on urban and fishery lights are restricted by the moonlight reflected by clouds, but the last applications of cloud distribution needs the lunar lights which are available for $\sim 1/2$ of the 29.5 day lunar cycle [8]. The optical properties of aerosol or cloud could be examined theoretically and empirically to provide and keep consistent data in those applications. The cloud properties were discussed for the nighttime observation and were estimated combining the light detected points and surroundings by DNB on the cloud free area, although the temporal and geometric variations need to be studied [11]. The quantitative retrievals of cloud optical depths exceeding values of 10 are now possible on moonlit nights, in which range the infrared signals may exhibit the saturation [8].

The possibility of SAR to validate the DNB data was discussed. And a temporal change of island building activities was studied using the mean intensity of DNB for a certain area of zone including islands and dredging activities.

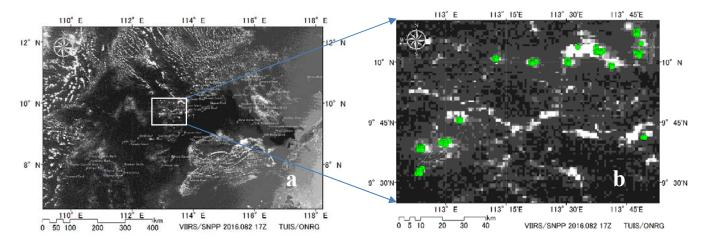


Fig. 2 DNB image on March 22, 2016, which was observed under the moon phase of waxing Gibbous with relative irradiance of 99 of the full moon (a), Fishery lights are empirically extracted (b)

II. APPROACH

A. Empirical Model to Extract Fishery Lights under Moon

An empirical approach was conducted to distinguish lights of fishing boats from lunar lights reflected by clouds as a function of brightness temperature (BT) at 3.7 μ m and DNB radiance, with an assumption that the strong lights of fishing boats may penetrate thin clouds [14].

The empirical equation was proposed from the regression line between DNB and $\Delta BT_{3.7}$, which is the detection limit as the temperature difference from the cloud free region at the given radiance of DNB.

$$\Delta BT_{3.7} = \exp(a \ DNB + b) \tag{1}$$

where a and b are empirical coefficients of 0.07 and 5.3, respectively. Operationally, the lights from the surface at the radiance of certain DNB (BT) could be distinguished from the cloud reflected lunar lights as:

$$BT_{3.7}^{max} > BT > BT_{3.7}^{max} - \Delta BT_{3.7}$$
 (2)

B. Validation with SAR Data

The Synthetic Aperture Radar data were applied to discuss a possibility of validating the DNB detected Scan SAR narrow mode A of Radarsat-2 on Dec. 8, 2014 at 10:25Z, of which spatial resolution is about 30 m by 30 m and its coverage is about 300 km by 300 km. The Scan SAR was selected because of its coverage, although the spatial resolution is not enough to observe a fine structures, but there is a possibility to identify microwave reflecting structures [12], [13]. Unfortunately, the SAR and DNB could not be synchronized because of the operational restriction, while the SAR needs the sufficient solar power energy which is not available in the night.

As the SAR image, once mapped on the GIS space, does not keep a concept of scan angle (column) and flight direction or azimuth (line), the SAR image was statistically analyzed based on the polygons prepared along scan lines of SAR image (Box polygons on Fig. 3). Fishery boats were identified from the

threshold defined by the higher scattering signals exceeding the multiple numbers of standard deviation within each polygons. This method was confirmed by the AIS data for 12 hours on the day when SAR observation was conducted.

C.Zone Statistics to Detect Temporal Change of Islands Activities

The DNB imagery was used to detect the temporal change of island building activities. Although the empirical method to identify lights from fishing boats under the lunar lights reflected by clouds was proposed in this study, the lunar lights-free data were selected to eliminate lights other than those from island-building activities in this analysis.

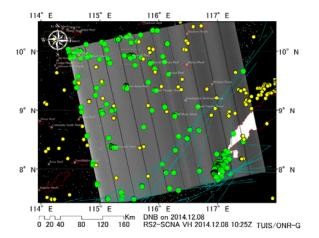


Fig. 3 Overlay of DNB detected fishery lights (small circle ●) on Dec. 8, 2014 at 17:28Z, Scan-SAR detected fishery boats (large circle ●) on Dec. 8, 2014 at 10:25Z, and cruise tracks (line ---) estimated from AIS data

Temporal changes in lights from activity around the islands were monitored with a mean intensity of DNB over a zone defined as a circular area. The circular areas were selected to capture lights from the islands as well as lights from the dredgers working around the islands.

The radius of each circle was scaled to 5 km, enclosing 78.5 km², which covers the runway and dredgers working around the island. The ArcMAP zonal statistics function was applied to get a DNB mean intensity from each circle zones. As clouds are not distributed uniformly within a scene, finding cloud free condition on one reef does not mean an equally cloud free for other reefs. Several days before and after the new moon were used when, on the actual day of the new moon, clouds obscured the ground and the received lights intensity was close to zero.

III. RESULTS

A. Fishery Lights Detected among Lunar Reflected Lights by Clouds

Fig. 2 (a) shows the DNB data on March 22, 2016, where fishery lights and lunar lights reflected by clouds are observed within one screen. The moon phase was the waxing Gibbous with the relative irradiance of 99% of the full moon. The empirical method proposed in this study was applied and the lights from fishing boats were extracted on Fig. 2 (b). The empirical method made it possible to identify the fishery lights from the lunar lights reflected by clouds.

B. Validation with SAR Data

Fig. 3 shows the fishery lights detected by DNB (small circle) on Dec.8, 2014 at 17:28Z and ships identified by SAR (large circle) on Dec.8, 2014 at 10:25Z. The locations of some ships detected by SAR were confirmed with the Automatic Identification System (AIS) dataset, where the locations of ships detected by SAR were interpolated from two locations of ships reported by AIS. The time difference between the DNB and the SAR observations made it difficult to validate the locations of fishery boats detected by the DNB with SAR, except the stable light sources on the islands.

C.Zone Statistics to Detect Temporal Change of Islands' Activities

Data from Mischief Reef (Fig. 4) showed a DNB mean intensity at or near 0 nW cm⁻² sr⁻¹ until January of 2015. The DNB mean intensity then increased gradually up to 6 nW cm⁻² sr⁻¹ from February of 2015 to June of 2015, and then to 10 nW cm⁻² sr⁻¹, observed in November of 2016, although month-to-month variations were observed. According to the CSIM/AMTI report, reclamation operations started in January of 2015, which corresponds to the period of increased DNB mean intensity. The DNB mean intensity increased gradually to higher level in June of 2015, around the time that the AMTI imagery showed the finished coastline. The highest DNB mean intensity around, 15 nW cm⁻² sr⁻¹, was observed in August of 2016, following to the first use of the runway by a civilian plane here, as well as at Subi Reef, in June of 2016.

IV. CONCLUSION & DISCUSSION

Although the validation is necessary for the empirical method to discriminate fishery lights from cloud reflected lunar lights, the time series of fishery lights may suggest one way to validate the empirical method to detect fishery lights. Or, an intensive studies on the light sources on the islands under

various cloud coverage and lunar illumination will give the validation data for the empirical method.

SAR data is the finest method to validate the locations of fishery lights and ships, if the synchronized observations between systems are possible. Unfortunately, the time lag around 6 hours between DNB and SAR observations made it difficult to validate DNB observation. The validation of stable light sources on islands or drifting ships could be possible and the intensive case study will be conducted.

The radius of circular area determines a sensitivity of DNB mean intensity. The current radius of 5 km covers the 3000 m airstrips and related activities, which covers all necessary activities. But the 5 km radius is too big for activities on or around smaller islands, because of large area of back ground. The intensive studies on the sensitivity of accounting zone and consistency are necessary, especially while comparing among different area of islands.

The DNB of VIIRS band on Suomi-NPP is a useful tool for monitoring island activities from the beginning of the dredging and following activities on constructions of buildings and/or runways.

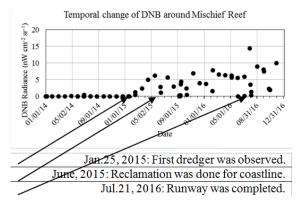


Fig. 4 Time series of DNB mean intensity of Mischief Reef from 2014 to 2016 with remarks read from satellite and reported

ACKNOWLEDGMENT

This research is partly supported by the Office of Naval Research Global of the USA with the grant number of N62909-15-1-2074. Authors appreciate Naval Research Laboratory of the USA for making the related data available for this project.

REFERENCES

- [1] Nguyen-Dang T., Fisheries Cooperation in the South China Sea and the (Ir)relevance of the Sovereignty Question, Asian Journal of International Law, 2 (1), 59-88 (2012)
- [2] Wessel, P., and W. H. F. Smith, A Global Self-consistent, Hierarchical, High-resolution Shoreline Database, J. Geophys. Res., 101, B4, 8741-8743 (1996).
- [3] Kyba, C. C. M., Garz, S., Kuechly, H., Miguel, A. S. de, Zamorano, J., Fischer, J., and Hölker, F., "High-Resolution Imagery of Earth at Night: New Sources, Opportunities and Challenges," *Remote Sens.* 7, 1-23 (2015).
- [4] Ma, S., Yan, W., Huang, Y., Ai, W., and Zhao, X., "Vicarious calibration of S-NPP/VIIRS day-night band using deep convective clouds," Remote Sens. of Env. 158, 42-55 (2015).

- [5] Cao, C. and Bai, Y., "Quantitative Analysis of VIIRS DNB Nightlight Point Source for Light Power Estimation and Stability Monitoring," Remote Sens. 6, 11915-11935 (2014).
- [6] Mazor, T., Levin, N., Possingham, H. P., Levy, Y., Rocchini, D., Richardson, A. J., "Can satellite-based night lights be used for conservation? The case of nesting sea turtles in the Mediterranean," Biological Conservation 159, 63-72 (2013).
- [7] Levin, N., Duke, Y., "High spatial resolution night-time light images for demographic and socio-economic studies," Remote Sens. of Env. 119, 1-10 (2012).
- [8] Miller, S. D., Straka, W., Mills, S. P., Elvidge, C. D., Lee, T. F., J. Solbrig, J., Walther, A., Heidinger, A. K., and Weiss, S. C., "Illuminating the Capabilities of the Suomi National Polar-Orbiting Partnership (NPP) Visible Infrared Imaging Radiometer Suite (VIIRS) Day/Night Band," Remote Sens. 5, 6717-6766 (2013).
- [9] Miller, S. D., Millsb, S. P., Elvidgec, C. D., Lindseyd, D. T., Lee, T. F., and Hawkins, J. D., "Suomi satellite brings to light a unique frontier of nighttime environmental sensing capabilities," Proc. National Academy of Sciences of the United States of America 109, 15706-15711 (2012).
- [10] Straka, W. C., Seaman, C., Baugh, K., Cole, K., Stevens, E., Miller, S. D., "Utilization of the Suomi National Polar-Orbiting Partnership (NPP) Visible Infrared Imaging Radiometer Suite (VIIRS) Day/Night Band for Arctic Ship Tracking and Fisheries Management," Remote Sens. 7, 971-989; doi:10.3390/rs70100971 (2015).
- [11] Elvidge, C. D., Zhizhin, M., Baugh, K., and Hsu, F., "Automatic Boat Identification System for VIIRS Low Light Imaging Data," Remote Sens. 7, 3020-3036; doi:10.3390/rs70303020 (2015).
- [12] Marino, A., M. J. Sanjuan-Ferrer, I. Hajnsek and K. Ouchi, Ship Detection with Spectral Analysis of Synthetic Aperture Radar: A Comparison of New and Well-known Algorithms, Remote Sens., 7, 5416-5439 (2015).
- [13] Wei, J., J. Zhang, G. Huang and Z. Zhao, On the Use of Cross-Correlation between Volume Scattering and Helix Scattering from Polarimetric SAR Data for the Improvement of Ship Detection, Remote Sens., 8, 74 (2016).
- [14] Asanuma, I., T. Yamaguchi, J. G. Park, K. Mackin, J. Mittleman, Detection of fishing boats by the day night band (DNB) on VIIRS, Imaging Spectrometry XXI, Proc. of SPIE, 9976, 99760P (2016).